Catalytic methanol decomposition over palladium deposited on mesoporous cerium oxide

Mahendra P. Kapoor [a,†], Yuichi Ichihashi [a], Koji Kuraoka [a], Wen-Jie Shen [a,‡], and Yasuyuki Matsumura [b,*]

[a] *National Institute of Advanced Industrial Science and Technology, Midorigaoka, Ikeda, Osaka 563-8577, Japan*
[b] *Research Institute of Innovative Technology for the Earth, Kizu-cho, Soraku-gun, Kyoto 619-0292, Japan*

Received 4 December 2002; accepted 17 March 2003

Ultrafine palladium particles can be deposited on mesoporous cerium oxide by a deposition–precipitation method. After reduction with hydrogen at 300 °C, palladium on the mesoporous compound is cationic with a valence close to +1 whereas the particles have a metallic structure. The catalytic activity in selective methanol decomposition to hydrogen and carbon monoxide at 180 °C is significantly higher than that of palladium supported on non-porous cerium oxide, suggesting that the mesoporous structure is advantageous to the reaction. When the palladium content is high, part of mesopores are probably choked with large palladium particles, which will cause saturation of the activity.

KEY WORDS: mesoporous cerium oxide; catalyst support; cationic palladium species; methanol decomposition; EXAFS.

1. Introduction

Methanol is expected to provide an alternative energy carrier to liquefied natural gas, hence improvements in the production and utilization of methanol are required. Methanol decomposition to carbon monoxide and hydrogen is applicable to the energy recovery of the waste heat from a methanol-fueled automobile in which the decomposition gas is supplied to the engine [1]. This endothermic reaction is expected to be applicable to heat recovery from various industries, but new catalysts active at low temperatures below 200 °C are required [2]. Palladium is an active catalyst in the reaction, and active palladium species can be produced by strong interaction with supports such as cerium oxide, especially when the catalyst is prepared by the deposition–precipitation method [3–8].

Silicic MCM-41 mesoporous materials have often been employed as catalyst supports and significant improvements in the activity have been reported, probably because the catalytic metals can be dispersed in the characteristic pore structure with high surface area [9]. It was found that mesoporous compounds of silica, titanium oxide, and zirconium oxide are effective supports of palladium for methanol decomposition [10–12]. Terribile *et al.* reported the preparation of mesoporous cerium oxide with a surface area of $\sim$200 m^2/g employing cetyltrimethylammonium bromide as a surfactant [13]. In this paper, we show that this compound can be synthesized from hexadecyltrimethylammonium bromide as the surfactant and it is an effective support of palladium.

2. Experimental

Mesoporous cerium oxide (CeO_2-MS) was synthesized from aqueous solutions of cerium sulfate octahydrate (25.6 mmol in 32 g of water) and hexadecyltrimethylammonium bromide (14 mmol in 175 g of water). The mixture was stirred at room temperature for 3 h, then the precipitate formed was aged at 100 °C for 4 days. The solid was filtered and washed with distilled water, then dried in air at 100 °C for 1 day. Finally, it was calcined in air at 350 °C for 5 h.

Palladium was deposited on the synthesized mesoporous cerium oxide or a commercial cerium oxide (Daiichi Kigenso Kagaku Kogyo, 98 m^2/g) by the deposition–precipitation method [14]. The oxide was dispersed in a 0.01 M HCl solution of palladium chloride ($PdCl_2$, Kishida Chemicals), then palladium hydroxide was exclusively precipitated on the surface of the support by gradual addition of 1 M Na_2CO_3 aqueous solution to the palladium solution heated at 70 °C with continuous stirring. The pH of the solution was maintained at 10 for 1 h. The resulting solid was filtered and washed with distilled water. The sample was dried at 120 °C overnight and calcined in air at 350 °C for 3 h. The mesoporous samples (*n* wt% Pd/CeO_2-MS, where *n* represents the palladium content) contained 1–10 wt% of palladium, and the nonporous samples (*n* wt% Pd/CeO_2) contained 3–5 wt% of palladium. Other mesoporous samples

* To whom correspondence should be addressed.
† Present address: Toyota Central R&D Laboratories Inc., Nagakute, Aichi 480-1192, Japan.
‡ Present address: Dalian Institute of Chemical Physics, Chinese Academy of Sciences, Zhongshan Road, Dalian 116023, China.
E-mail: yasuyuki@rite.or.jp

1011-372X/03/0500-0083/0

(n wt% Pd/CeO_2-MS-U) were also prepared in an ultrasonic vibration bath maintained at 70 °C during the process of palladium deposition.

Powder X-ray diffraction (XRD) patterns of the samples were recorded with a Rigaku Rotaflex 20 diffractometer using nickel-filtered Cu K_α radiation. The distribution of the pore diameter was determined from the adsorption and desorption isotherms of nitrogen obtained with a BELSORP 28 instrument (BEL, Japan). The BET surface areas of the samples were determined from the isotherms of nitrogen physisorption.

Catalytic reaction was performed in a fixed-bed continuous-flow reactor under atmospheric pressure. A catalyst (0.20 g) diluted with 1.0 g of quartz sand, being inert under the reaction conditions, was sandwiched with quartz-wool plugs in a quartz tube reactor of 6 mm i.d. The samples were reduced in a flow of 20 vol% hydrogen diluted with argon (flow-rate, 9.6 dm^3/h) for 1 h at 300 °C, then 20 vol% of methanol was fed with an argon carrier (total flow-rate 4.8 dm^3/h) at 180 °C. The outlet gas was analyzed with an on-stream gas chromatograph (Yanagimoto G2800) equipped with a Porapak-T column (4 m) and a thermal conductivity detector.

X-ray photoelectron spectra (XPS) were recorded at room temperature with a Shimadzu ESCA 750 instrument. After being reduced with hydrogen (20 kPa) at 300 °C for 1 h in a vacuum line, the well-ground sample was mounted in air in a sample holder. In order to remove surface adsorbates, Argon ion sputtering for 0.5 min at 2 kV and 20 mA was carried out just before the measurement. Binding energies were corrected by reference to the C 1s line at 284.6 eV.

Profiles of extended X-ray absorption fine structure (EXAFS) for the samples were taken at room temperature in the transmission mode for K-edges of Pd at beamline BL01B1 of SPring-8. The samples were reduced with hydrogen (20 kPa) at 300 °C for 1 h in a vacuum line and sealed with polyethylene films in a nitrogen atmosphere. Fourier transformation was performed on k^3-weighted EXAFS oscillations in the range 30–150 nm^{-1}. Normalization of the EXAFS function was done by dividing the absorption intensity by the height of the absorption edge. A cubic spline background subtraction was carried out. The inverse Fourier transform was obtained within windows 0.19–0.28 nm in r space. The Pd–Pd reference was derived from EXAFS of Pd foil. Analysis was performed with the program REX supplied by Rigaku.

3. Results and discussion

3.1. Structure of mesoporous cerium oxide

In the XRD pattern of the synthesized mesoporous cerium oxide, there were two peaks at 2.4 and 4.2° 2θ after calcination in air at 350 °C for 5 h (figure 1),

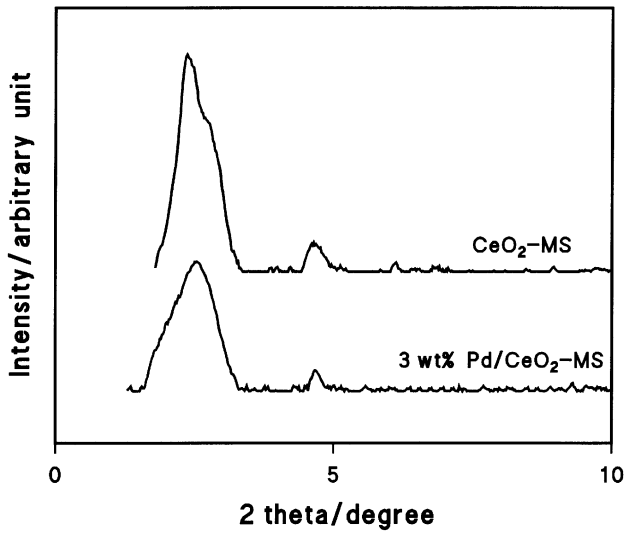

Figure 1. XRD patterns of mesoporous cerium oxide and that modified with palladium by the deposition–precipitation method.

showing successful synthesis of the cerium oxide with a mesoporous structure [15]. The peak at 2.4° is attributed to a lattice with a d-spacing of 3.7 nm.

The pore diameter of CeO_2-MS was distributed in the range 3–5 nm (the maximum was at 4.4 nm) with a pore volume of 93 mm^3/g (figure 2). The distribution changed after deposition of palladium. The pore diameter of the mesoporous compound containing 3 wt% of palladium (3 wt% Pd/CeO_2-MS) was sharply distributed around 3.6 nm and the volume was discernibly reduced to 80 mm^3/g while the volume of 3 wt% of palladium was 2.5 mm^3/g. The XRD peak originally at 2.4° slightly shifted to 2.5° 2θ, corresponding to a 3.5 nm spacing (see figure 1), and peak broadening was observed after the modification of palladium. This suggests that the crystalline structure of CeO_2-MS is basically retained after the modification of palladium, and it is not

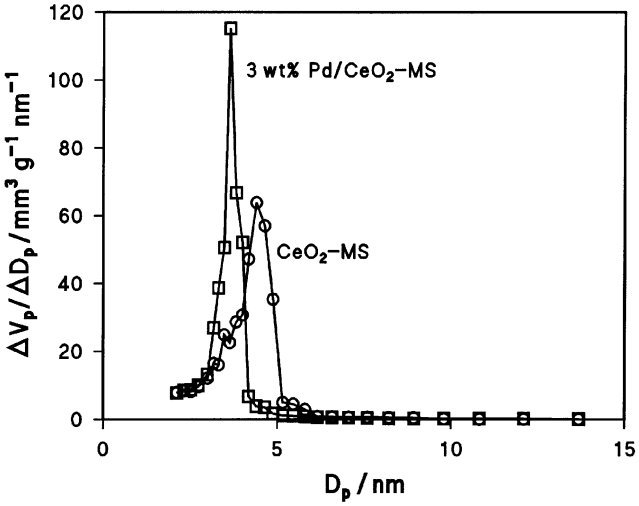

Figure 2. Pore-size distributions of mesoporous cerium oxide and that modified with palladium by the deposition–precipitation method. D_p, pore diameter; V_p, pore volume.

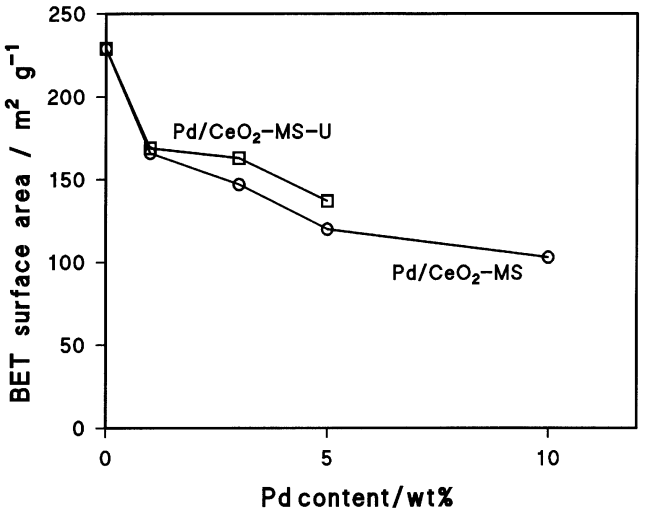

Figure 3. BET surface area of palladium supported on mesoporous cerium oxide.

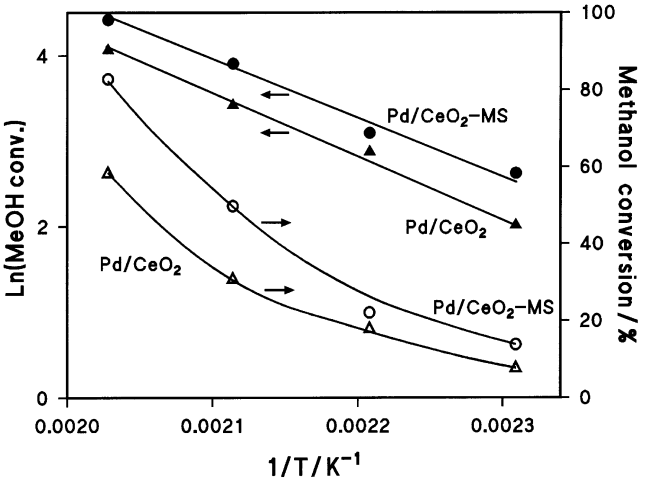

Figure 5. Temperature dependence of catalytic activity of palladium supported on mesoporous and non-porous cerium oxide for selective methanol decomposition. Palladium content, 3 wt%.

responsible for the change in pore-size distribution. Hence it is supposed that the presence of palladium particles in the mesopores reduces the effective pore size which is detected by the adsorption method. The BET surface area of CeO_2-MS was 229 m^2/g and it gradually decreased with increasing palladium content (figure 3).

3.2. Catalytic activity for methanol decomposition

The catalytic activity of Pd/CeO_2-MS in selective methanol decomposition to carbon monoxide and hydrogen at 180 °C was higher than that for Pd/CeO_2 (figure 4). The activity of Pd/CeO_2-MS-U, which was prepared by palladium deposition using ultrasonic vibration, was considerably larger than that of Pd/CeO_2-MS. No significant deactivation of the catalysts was observed during reaction for 6 h. The activity of 3 wt% Pd/CeO_2-MS was always higher than that of 3 wt% Pd/CeO_2 in the temperature range 160–220 °C (figure 5). The activation energies from the plots were 55 and 59 kJ/mol, respectively.

Since the catalytic activity of palladium for methanol decomposition depends on the electronic state of palladium which is detectable with the binding energy of Pd 3d [3–8], X-ray photoelectron spectra of Pd/CeO_2-MS were recorded. The binding energies of Pd $3d_{5/2}$ for 3, 5 and 10 wt% Pd/CeO_2-MS were 335.8 ± 0.1 eV (figure 6) and those of O 1s were 529.6 ± 0.1 eV. The energy of Pd $3d_{5/2}$ for 3 wt% Pd/CeO_2 was 335.9–336.2 eV [7,8] and that of metallic palladium was 335.0 eV [16]. Since the binding energy of Pd/CeO_2-MS is close to that of Pd/CeO_2, the palladium species on the mesoporous cerium oxide is similar to the species on the non-porous cerium oxide. Kili *et al.* reported that Pd $3d_{5/2}$ at 336.8 eV is attributable PdO in Pd/γ-Al_2O_3 modified with cerium or lanthanum oxide [17]. In the case of PdO/MgO the energy was reported to be 336.5 eV [18].

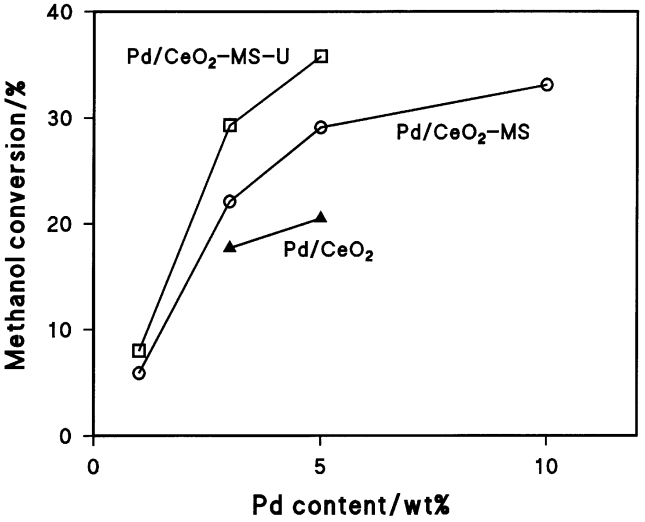

Figure 4. Catalytic activities of palladium supported on mesoporous and non-porous cerium oxide for selective methanol decomposition.

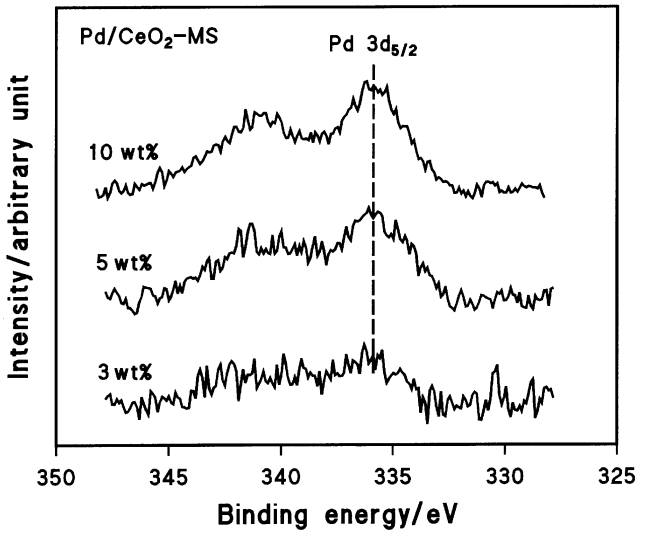

Figure. 6. XPS of Pd 3d region for palladium supported on mesoporous cerium oxide reduced at 300 °C.

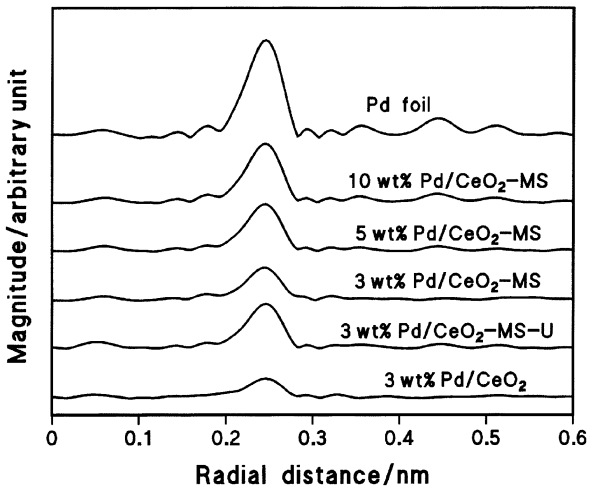

Figure 7. Fourier transforms of k^3-weighted Pd K-edge EXAFS for palladium supported on mesoporous and non-porous cerium oxide reduced at 300 °C.

Table 1
EXAFS parameters of Pd–Pd interaction for palladium supported on mesoporous and non-porous cerium oxide reduced at 300 °C

Sample	Interatomic distance, R (nm)	Coordination number, N	Debye–Waller factor, σ (nm)
Pd foil	0.275	12.0	0.0060
	0.476	24.0	0.0060
	0.550	12.0	0.0062
3 wt% Pd/CeO_2	0.273	5.2	0.0089
3 wt% Pd/CeO_2-MS-U	0.275	8.1	0.0075
	0.479	9.2	0.0077
	0.545	4.5	0.0082
3 wt% Pd/CeO_2-MS	0.274	6.6	0.0080
5 wt% Pd/CeO_2-MS	0.275	8.4	0.0074
	0.478	11.2	0.0080
	0.546	3.4	0.0082
10 wt% Pd/CeO_2-MS	0.275	9.5	0.0071
	0.477	14.9	0.0071
	0.545	4.9	0.0072

Hence the valence of the palladium species on the mesoporous oxide should be close to +1 and the palladium particles on mesoporous cerium oxide interact with the support as strongly as on the non-porous oxide. Since the activation energy for methanol decomposition depends on the electronic state of palladium, this finding is consistent with the reaction results.

In order to analyze the structure of palladium, EXAFS analyses were performed. The Fourier transforms of the Pd K-edge EXAFS for 3 wt% Pd/CeO_2-MS reduced at 300 °C for 1 h showed the presence of a peak at 0.24 nm (phase shift uncorrected), mainly attributed to Pd–Pd interaction, while the peak for 3 wt% Pd/CeO_2 was very weak (figure 7). The coordination number of the first Pd–Pd shell for 3 wt% Pd/CeO_2-MS determined by curve fitting was 6.6 and appreciably larger than that for 3 wt% Pd/CeO_2 (table 1). Since the coordination number depends basically on the number of atoms in a particle [19], the dispersion of palladium in 3 wt% Pd/CeO_2-MS is appreciably smaller than that for 3 wt% Pd/CeO_2. In general, activity relates to the dispersion of the catalytic metal. However, the activity of the former catalyst is larger than that of the latter while the results of XPS analysis show the presence of cationic palladium species in both the catalysts. Measurement of the palladium dispersion for the catalysts by hydrogen or carbon monoxide adsorption was not successful because of surface spill-over of the adsorbate to ceria [7,8].

In the case of 3 wt% Pd/CeO_2-MS-U, the activity of which is the highest of the three 3 wt% Pd samples, the coordination number was determined as 8.1, showing the lowest dispersion. The EXAFS parameters for the higher shells were not exact, but they were included in the calculation to increase the accuracy of the first-shell fitting (see table 1). The calculated curve of k^3-weighted Pd K-edge EXAFS oscillations fits the experimental data well (figure 8). The promotional effect of mesopores on the activity of palladium to methanol decomposition was found in the cases of mesoporous zirconium oxide [11] and mesoporous titanium oxide [12]. Since the walls of mesopores closely surround palladium particles, the concentration of methanol near palladium may increase by the interaction between methanol and the three-dimensional pores and this can enhance the decomposition of methanol. A similar effect was also observed with nickel supported on a porous glass the pore diameter of which is close to the size of nickel particles in the catalyst [19] but further elucidation is necessary to account for this phenomenon.

The prediction of particle size for metallic species from the coordination number has gained widespread use. The mean particle size of palladium in 3 wt% Pd/CeO_2-MS can be estimated as 0.8 nm on the basis of the standard procedure proposed by Greegor and Lytle assuming spherical

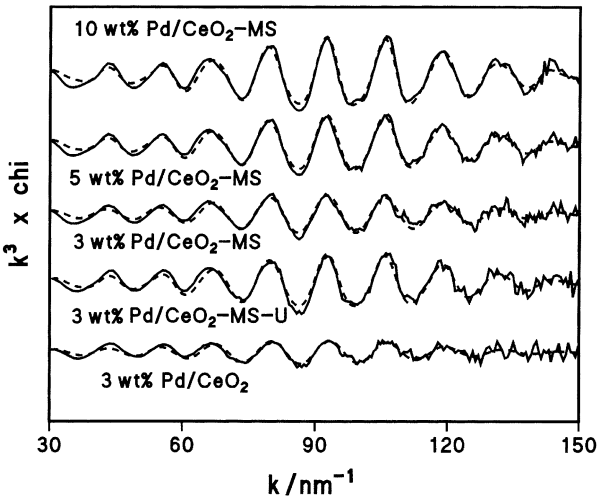

Figure 8. k^3-Weighted Pd K-edge EXAFS oscillations for palladium supported on mesoporous and non-porous cerium oxide reduced at 300 °C. Solid line, experimental data; broken line, calculated fit.

particles [19]. The presence of these small particles in the mesopores can account for the decrease in the pore diameter (see figure 2) without a significant change in *d*-spacing (see figure 1) after the modification of palladium. In case of 3 wt% Pd/CeO_2-MS-U, the mean particle size estimated by the standard method is 1.3 nm. Since the BET surface area of the sample is discernibly larger than that of 3 wt% Pd/CeO_2-MS, the larger particles in 3 wt% Pd/CeO_2-MS-U do not choke the mesopores as much as in 3 wt% Pd/CeO_2-MS. The mean particle size of 5 wt% Pd/CeO_2-MS is estimated as 1.4 nm and is almost the same as that for 3 wt% Pdsolidus;CeO_2-MS-U. Since the activities of both catalysts are almost the same, part of the palladium particles in 5 wt% Pd/CeO_2-MS should not contribute to the reaction. The mean particle size for 10 wt% Pd/CeO_2-MS is estimated as 1.9 nm. The Pd surface area of the sample is calculated as 26 m^2/g from this particle size, assuming spherical particles with an identical diameter. Although the area is considerably larger than that for 5 wt% Pd/CeO_2-MS (18 m^2/g), the activity of the 10 wt% catalyst is not as high as expected from the palladium area. The decrease in the BET surface area with increase in palladium content (see figure 3) suggests choking of the mesopores with palladium particles and this is probably the reason why the activity gradually becomes saturated with increasing Pd content (see figure 4). The higher activities and surface areas of Pd/CeO_2-MS-U than those of the corresponding Pd/CeO_2-MS samples show that ultrasonic vibration during the process of palladium deposition on the mesoporous ceria can reduce the extent of the choking of mesopores.

In conclusion, ultrafine palladium particles can be introduced into mesoporous cerium oxide by a deposition–precipitation method. The methanol decomposition is effectively catalyzed over palladium deposited in the mesopores and the activity is significantly higher than on a non-porous ceria support, showing that the pore structure affects the reaction. The activity of palladium in mesoporous oxide is gradually saturated with increasing palladium content, probably because large palladium particles partly choke the mesopores, while employment of ultrasonic vibration in the deposition process of palladium is effective in preventing the choking.

Acknowledgments

The synchrotron radiation experiment was performed with the approval of the Japan Synchrotron Radiation Research Institute (Proposal 2001A0083-NX-np). W.S. acknowledges a fellowship from the New Energy and Industrial Technology Development Organization of Japan.

References

[1] National Research Council, *Catalysis Look to the Future* (National Academy Press, Washington, DC, 1992).
[2] T. Nishimura, T. Omata and Y. Ogisu (eds.), *Eco-Energy City System* (in Japanese) (Energy Conservation Center, Tokyo, 1999).
[3] Y. Matsumura, M. Okumura, Y. Usami, K. Kagawa, H. Yamashita, M. Anpo and M. Haruta, Catal. Lett. 44 (1997) 189.
[4] Y. Usami, K. Kagawa, M. Kawazoe, Y. Matsumura, H. Sakurai and M. Haruta, Appl. Catal. A 171 (1998) 123.
[5] Y. Usami, K. Kagawa, M. Kawazoe, Y. Matsumura, H. Sakurai and M. Haruta, Stud. Surf. Sci. Catal. 118 (1998) 83.
[6] Y. Matsumura, Y. Ichihashi, Y. Morisawa, M. Okumura and M. Haruta, Stud. Surf. Sci. Catal. 130 (2000) 2315.
[7] W.-J. Shen and Y. Matsumura, Phys. Chem. Chem. Phys. 2 (2000) 1519.
[8] W.-J. Shen and Y. Matsumura, J. Mol. Catal. A 153 (2000) 165.
[9] C.A. Koh, R. Nooney and S. Tahir, Catal. Lett. 47 (1997) 199, and references therein.
[10] Y. Liu, K. Suzuki, S. Hamakawa, T. Hayakawa, K. Murata, T. Ishii and M. Kumagai, Catal. Lett. 66 (2000) 205.
[11] M.P. Kapoor, Y. Ichihashi, W.-J. Shen and Y. Matsumura, Catal. Lett. 76 (2001) 139.
[12] Y. Matsumura, M.P. Kapoor, Y. Ichihashi, H. Ando and K. Kuraoka, Catal. Catal. 42 (2000) 363.
[13] D. Terribile, A. Trovarelli, J. Llorca, C. de Leitenburg and G. Dolcetti, J. Catal. 178 (1998) 299.
[14] W.-J. Shen, M. Okumura, Y. Matsumura and M. Haruta, Appl. Catal. A 213 (2001) 225.
[15] S. Biz and M.L. Occelli, Catal. Rev. Sci. Eng. 40 (1998) 329.
[16] D. Briggs and M.P. Seah (eds.) *Practical Surface Analysis*, Vol. 1: *Auger and X-ray Photoelectron Spectroscopy*, 2nd edition (Wiley, New York, 1990).
[17] K. Kili, L. Hilaire and F. Le Normand, Phys. Chem. Chem. Phys. 1 (1999) 1623.
[18] A. Ogata, A. Obuchi, K. Mizuno, A. Ohi and H. Ohuchi, J. Catal. 144 (1993) 452.
[19] R.B. Greegor and F.W. Lytle, J. Catal. 63 (1980) 476.